

# Structure-dynamics relation in physically-plausible multi-chromophore systems

George C. Knee,<sup>\*,†</sup> Patrick Rowe,<sup>‡,¶</sup> Luke D. Smith,<sup>†</sup> Alessandro Troisi,<sup>‡</sup> and Animesh Datta<sup>\*,†</sup>

<sup>†</sup>*Department of Physics, University of Warwick, Coventry CV4 7AL, United Kingdom*

<sup>‡</sup>*Department of Chemistry, University of Warwick, Coventry CV4 7AL, United Kingdom*

<sup>¶</sup>*London Centre for Nanotechnology, Thomas Young Centre, and Department of Physics and Astronomy, University College London, 17-19 Gordon Street, London WC1H 0AH, UK*

E-mail: gk@physics.org; animesh.datta@warwick.ac.uk

## Abstract

We study a large number of physically-plausible arrangements of chromophores, generated via a computational method involving stochastic real-space transformations of a naturally occurring ‘reference’ structure, illustrating our methodology using the well-studied Fenna-Matthews-Olsen complex (FMO). To explore the idea that the natural structure has been tuned for the efficient transport of excitons, we use an atomic transition charge method to calculate the excitonic couplings of each generated structure and a Lindblad master equation to study the quantum transport of an exciton from a ‘source’ to a ‘drain’ chromophore. We find statistically significant correlations between structure and transport efficiency: High-performing structures tend to be more compact and, among those, the best structures display a certain orientation of the chromophores, particularly the chromophore closest to the source-to-drain vector. We conclude that, subject to reasonable, physically-motivated constraints, the FMO complex is highly attuned to the purpose of energy transport, partly by exploiting these structural motifs.

## Introduction

The process of excitonic energy transport is of great interest across many fields of study, from evolutionary biology to the engineering of solar cells. It is a key component of both natural photosynthesis (occurring in light harvesting complexes (LHCs), which are assemblages of chromophores found in a famously ‘warm and wet’ environment) and artificial photovoltaics. It is tempting to suggest that, since natural selection has had perhaps billions of years<sup>1</sup> over which to improve the efficiency of the process, we might learn from nature how to better engineer artificial light harvesting systems. This view has gathered interest in recent years, in tandem with claims that naturally occurring systems can exhibit outstandingly high efficiency.<sup>2,3</sup> It is often said that quantum coherence could play a pivotal role in enhancing transport<sup>4-7</sup> through constructive interference of excitation pathways (although this is hotly debated<sup>8-10</sup>) and that the structural arrangement of chromophores has been optimised for this functionality.<sup>3</sup> Contrariwise, it might be suggested that efficient transport through a network of chromophores is actually generic and most of the possible structural arrangements would show similar performance. It is difficult to draw conclusions about the general structure-dynamics

relationship from studying only a handful of naturally occurring LHCs. Indeed, while it is clearly desirable to learn from the results of natural selection,<sup>11</sup> we must also be able to relax the constraints that it operated under in order to uncover the potential for technological advantage, while at all times keeping our imagination on a short enough leash so that any new structures remain physically plausible.

Theoretical efforts have so far proceeded along two paths. The first technique is to randomly ‘sprinkle’ point-like electrical dipoles into a restricted volume: This approach has allowed the use of genetic algorithms to optimise their positions,<sup>12</sup> and later showed how fast transport is typically aided by a ‘backbone plus pair’ geometry by reinforcing constructive interference,<sup>13</sup> and correlated to the centrosymmetry of the Hamiltonian describing the energy of the system.<sup>14</sup> The spatial density of dipoles was considered,<sup>15</sup> and (although generally correlated with efficient exciton transport) was found to saturate to the densities typically found in natural LHCs.<sup>16</sup> A drawback of such approaches is that they may not have much to say about realistic systems, whose structure and properties are determined by more complicated, highly-constrained relations between anisotropic molecules extended in physical space.

The second technique begins with a commonly accepted mathematical model of an existing system, and performs perturbations on it. This approach has enabled investigations of robustness and identification of dominant transport pathways in a naturally occurring LHC,<sup>17</sup> as well as transport efficiency in purple bacteria compared with counterfactual structures, obtained through rotating<sup>10</sup> or ‘trimming’<sup>18</sup> chromophores from the LH1 and LH2 complexes. The latter works speculate on the relative importance of coherent supertransfer in these systems (noting that it is a ‘spandrel’ – or evolutionary byproduct – rather than an adaption) as well as the degree of attunedness of the original structure for energy transport. A possible drawback of these approaches, as we explain below, is the potential physical implausibility of the perturbed models, especially when

the transformations involve ‘deleting’ coupling terms or making uncorrelated perturbations to the Hamiltonian matrix. Other strategies deploy abstract models of the transport system<sup>19–23</sup> to learn general principles from idealised ‘network’ models that may operate to a greater or lesser extent in realistic systems.

In this Letter, we incorporate the best of the above strategies to address two key questions on the structure-dynamics relationship for exciton transport: (i) which structural motifs influence exciton dynamics in typical physically-plausible multi-chromophore complexes? and (ii) do naturally occurring complexes appear to be attuned for certain transport tasks (by exploiting these motifs or otherwise)? We proceed by simulating the transport properties of a large number of artificial, or *ersatz* structures obtained from a reference one by geometrical perturbations (GPs). We illustrate our methodology by considering the efficiency of excitonic transport in the FMO, but it can just as well be applied to any LHC and any performance metric.

## Generation of ersatz structures and model Hamiltonians

We generate a sample of plausible structures, associating to each an  $N \times N$  Hamiltonian matrix representing a network of  $N$  chromophores where a single excitation can exist. We take the naturally occurring Fenna-Matthews-Olsen (FMO) complex<sup>24</sup> as our reference structure, chosen for its simplicity and relevance as a model system for LHCs.<sup>25</sup> Present in species of green sulfur bacteria, the complex takes the form of three identical protein monomers, each of which comprising a protein matrix which contains  $N = 8$  identical bacteriochlorophyll-*a* (BChl) chromophores<sup>26</sup> (see Fig. 1). As we will be interested in exciton transport between BChls 1 (‘source’, closest to the antenna) and 3 (‘drain’, closest to the reaction centre), we fix their position, while the other 6 BChls are rigidly displaced and rotated by a sequence of  $n = 50,000$  Monte-Carlo moves, starting with their reference locations (see supplementary information).<sup>27–29</sup> During the GP, we retain only

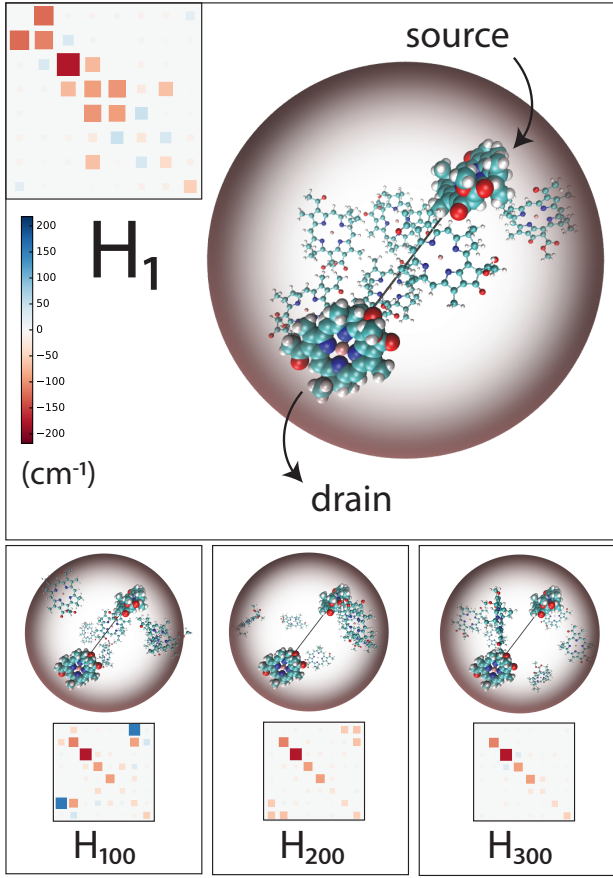


Figure 1: The FMO trimer is composed of three (monomer) subunits, each consisting of eight BChl chromophores supported in a protein scaffolding. We consider a single unit of the complex, where the protein is retained only implicitly through its role as a dielectric and vibrational environment. Observe our enclosing sphere, which all chromophores must fit within, and the ‘transport vector’ which connects BChls 1 and 3 (enlarged for clarity), which serve as source and drain respectively. We generate 50,000 new structures through physical changes to the FMO. Three representative structures are shown, along with their resulting Hamiltonian matrices (in the chromophore basis) which we calculate using an Atomic Transition Charge method. To aid clarity, the energies of all BChls have been shifted such that the energy of BChl 1 is zero.

plausible *ersatz* structures by rejecting those where the minimum inter-atomic separation between the BChls is smaller than  $d_{\min} = 2\text{\AA}$ , a cut-off intermediate between bonding and van der Waals distances; and contain the geometric

centroid of each BChl within a sphere of radius  $r_{\max} = 22.3\text{\AA}$  from the midpoint between BChls 1 and 3 (roughly representing the volume contained by the protein matrix in the reference structure).

To each *ersatz* structure  $i$  we associate the excitonic Hamiltonian

$$H_i = \sum_{l=1}^{N=8} \epsilon_l |l\rangle\langle l| + \sum_{m \neq n} V_{mn}^{(i)} (|m\rangle\langle n| + |n\rangle\langle m|). \quad (1)$$

This expression is written with respect to an orthonormal set of basis states  $|l\rangle$ , each representing the situation where BChl  $l$  is excited and all other BChls are not. The diagonals  $\epsilon_l$  represent the energy landscape for non-interacting chromophores. While some previous studies set their distribution to be uniform,<sup>12</sup> we retain a non trivial distribution by fixing the diagonals to those corresponding to the reference FMO (see supplementary information). An energy gradient, aided by a bath-mediated relaxation, can ‘funnel’ excitations towards lower-lying excited states. Although our modelling of the bath forbids this relaxation, we argue that these ‘site’ energies can be nevertheless very influential on the exciton dynamics. They determine the energy eigenstates of  $H_i$  and therefore influence the phase relationship and subsequent interference between different pathways through the network.

The off-diagonal elements  $V_{mn}^{(i)}$  arise from Coulomb interactions between transition charge densities, and depend on the mutual orientation of the chromophores. It is well known that a simple point-dipole approximation to  $V_{mn}^{(i)}$  would break down at the short distances we consider:<sup>30</sup> we therefore adopt a superior approach,<sup>31</sup> partitioning the atomic transition density for each structure  $i$  into atomic transition charges  $q_{\alpha m}^t$  (with coordinates  $\mathbf{R}_{\alpha m}^{(i)}$ ) centred on atom  $\alpha$  of chromophore  $m$ . The Coulombic interaction is then summed to evaluate the coupling

$$V_{mn}^{(i)} = f \sum_{\alpha}^{N_a} \sum_{\beta}^{N_b} \frac{q_{\alpha m}^t q_{\beta n}^t}{|\mathbf{R}_{\alpha m}^{(i)} - \mathbf{R}_{\beta n}^{(i)}|}. \quad (2)$$

## Quantum dynamics model

We use a phenomenological dynamical model for the motion of a single exciton through our network of chromophores. While several more elaborate models exist,<sup>32</sup> our Lindblad master equation captures the essential effects of dephasing and dissipation, and represents a completely positive transformation<sup>33</sup> on the density matrix  $\rho$ . Defining  $\mathcal{L}(\rho) \equiv L\rho L^\dagger - \frac{1}{2}\{L^\dagger L, \rho\}$ , we have

$$\dot{\rho}_i = -i[H_i, \rho_i] + \mathcal{L}^{\text{sink}}(\rho_i) + \sum_{j=1}^8 [\mathcal{L}_j^{\text{deph}}(\rho_i) + \mathcal{L}_j^{\text{diss}}(\rho_i)]. \quad (3)$$

The first term represents closed-system dynamics, and the other terms represent effects arising from interaction with an environment, with the collapse operators taken to be independent of the structure index  $i$  and given by

$$\begin{aligned} L^{\text{sink}} &= \sqrt{2\Gamma^{\text{sink}}} |\text{sink}\rangle\langle 3|; & \Gamma^{\text{sink}} &= 6.3\text{ps}^{-1} \\ L_j^{\text{deph}} &= \sqrt{2\Gamma_j^{\text{deph}}} |j\rangle\langle j|; & \Gamma_j^{\text{deph}} &= 2.1\text{ps}^{-1} \\ L_j^{\text{diss}} &= \sqrt{2\Gamma_j^{\text{diss}}} |\text{env}\rangle\langle j|; & \Gamma_j^{\text{diss}} &= 0.0005\text{ps}^{-1}. \end{aligned} \quad (4)$$

We have expanded the Hilbert space to include  $|\text{sink}\rangle$  and  $|\text{env}\rangle$  (environment) which are states accessible through dissipation but which cannot build up any coherence with the rest of the network. Here,  $\mathcal{L}^{\text{sink}}$  is a fast and irreversible process that represents successful capture of the exciton at BChl 3, where it is transferred to a reaction centre, or ‘sink’.<sup>1</sup> Otherwise, here all incoherent processes operate independently of the chromophore index  $j$ .  $\mathcal{L}^{\text{diss}}$  represents the relatively slow process of exciton dissipation (or decay). The  $\mathcal{L}_j^{\text{deph}}$  term represents the averaged coupling of BChl  $j$  to its vibrational environment, leading to a local loss of coherence. If this happens too quickly, the exciton can be ‘frozen’ and prevented from evolving as per the Zeno effect.<sup>34</sup> If dephasing is too slow, destructive interference can lock the exciton in a particular subspace.<sup>20</sup> We choose rates extracted from spectroscopy experiments at 77K,<sup>35</sup> but our

conclusions are robust to moderate changes in these values (see supplementary information).

Although the choice of a realistic initial condition for the exciton transport is the subject of some debate,<sup>36</sup> we set  $\rho_i(0) = |1\rangle\langle 1|$ , an exciton localised on BChl 1 (our ‘source’). This is consistent with the accepted photo-excitation process, which occurs in the nearby chlorosome (which acts as an antenna<sup>1</sup>). We numerically solve the Lindblad master equation for  $\rho_i(t)$ , which can be thought of as a Hilbert-space operator ‘trajectory’ associated with each *ersatz* structure. It is this association which will allow us to explore the structure-dynamics relationship.

## Structure-dynamics relationships

First we consider how compact the chromophores are along the ‘transport vector’ which connects the source and drain (see Fig. (1)). Define

$$M_i \equiv \sum_{k \in \text{Mg}} (r_k^{(i)})^2, \quad (5)$$

(the mass-normalised moment of inertia), where  $r_k^i$  is the perpendicular distance of each atom in structure  $i$  to the transport vector and the sum is taken only over the coordinates of the Magnesium atoms that lie roughly in the centre of each BChl. Fig. (2a) shows that the vast majority of our sample has  $M_i > M_1$ . We infer that it is difficult to pack the BChls into a volume smaller than nature has, without having unreasonably short distances between chromophores. We will return to this point later on.

Our focus is on investigating the structural properties of those randomly generated structures which perform ‘best’ at some exciton transport function, e.g. fast or high-yield transport; high-retention storage or even fast energy-dissipation. Those structures performing well can be inspected for characteristics which might form the basis of design principles for synthetic applications. Here, we quantify the performance of our dynamics via the transport efficiency

$$\eta_i(t) \equiv \langle \text{sink} | \rho_i(t) | \text{sink} \rangle, \quad (6)$$

which measures both the speed and yield of en-

ergy transfer.

To identify the main structural motifs influencing the exciton dynamics we use the Spearman rank correlation coefficient  $\mathcal{S}(x, y)$ . Ranging between  $-1$  and  $+1$ , the coefficient measures the extent to which two quantities  $x$  and  $y$  are monotonically related (see supplementary information). In this work, we fix  $x = \eta_i(t)$ , and begin with  $y = M_i$ . Fig. (2c,e) shows an inverse correlation between the moment of inertia  $M_i$  and the transport efficiency  $\eta_i(t)$ . More compact structures tend to exhibit faster transport.

In fact, this realisation has a bearing on the second of our key questions (ii): To investigate the relative performance of the reference structure, we introduce the normalised rank (henceforth ‘rank’)  $\mathcal{R}_x$  defined as

$$\mathcal{R}_x \equiv 1 - o(x)/N, \quad (7)$$

where  $o(x) \in \{1, \dots, n\}$  is the ordinal rank by measure  $x$  through our sample of *ersatz* structures. Thus, at time  $t$ , the reference structure has  $\mathcal{R}_\eta$  equal to one (zero) if it has the highest (lowest)  $\eta_i(t)$  among all *ersatz* structures in the sample. A rank of 0.5 means there are as many *ersatz* structures outperforming as underperforming the reference. The standard deviation of  $\eta$  is written as  $\sigma(\eta)$ : this gives an idea of the overall variation in transport efficiencies exhibited by our sample of structures. If  $\sigma(\eta)$  is small, then a high rank may correspond to a small increase in efficiency in absolute terms. Likewise a large deviation hints that there is more variation in the sample, and more efficiency at stake for high ranking structures to benefit from.

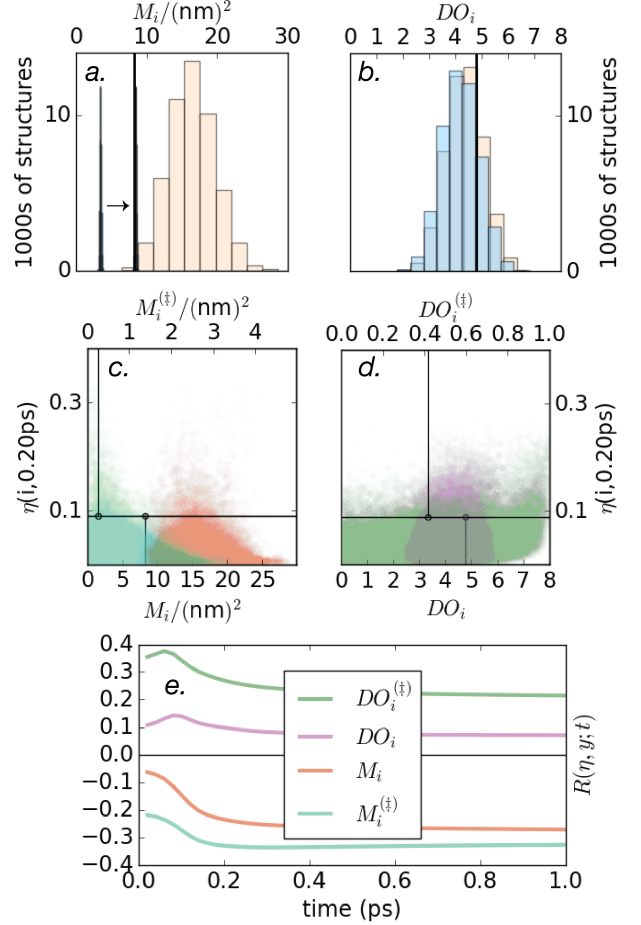


Figure 2: The upper panels show histograms for a) moment of inertia ( $M_i$ ) and b) dipole orientation ( $DO_i$ ) of the geometric perturbation (GP, peach) and rotations only (GP(R), blue) sample of structures. Reference values  $M_1$  and  $DO_1$  are shown with thick black lines. In panel a) the very narrow histogram for GP(R) has been shifted by 5 (nm)<sup>2</sup> for clarity. The middle panels show scatter plots of our structural properties versus transport efficiency at 0.2 ps. One can visualise c) a negative correlation with moment of inertia  $M_i$  (orange, bottom axis), and a stronger negative correlation with the key moment of inertia  $M_i^{(\ddagger)}$  (turquoise, top axis); and d) a positive correlation with  $DO_i$  (purple, bottom axis) along with a stronger positive correlation with the key dipole orientation  $DO_i^{(\ddagger)}$  (green, top axis). In pane d), we have frozen the moment of inertia of all structures to be that of the reference  $M_i \rightarrow M_1$ . In each pane, the data point for the reference structure is shown with a black crosshair. These time-resolved correlations are shown in panel e). Note the separation of timescales: up to about  $1/2\Gamma^{\text{deph}} \sim 250\text{fs}$ , the correlations change rapidly before stabilising.

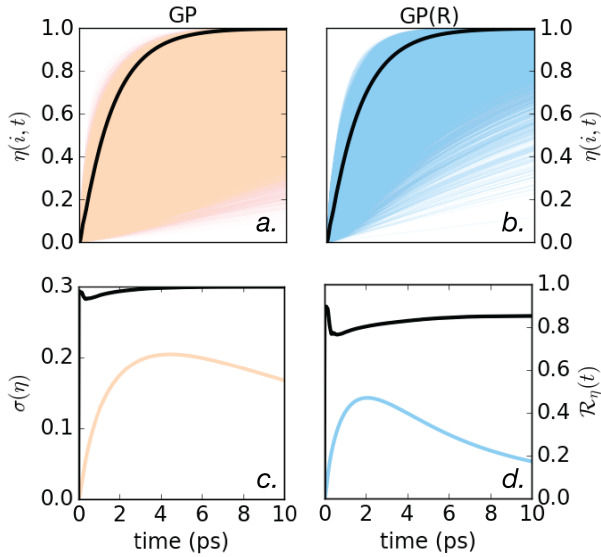


Figure 3: The upper panels show exciton transport efficiency over time for a) all structures generated with geometric perturbation (GP) method (peach) and b) all structures generated with rotations only (GP(R)) method (blue). In both cases the reference FMO structure is shown with a thick black line. The lower panels show the deviation in efficiency  $\sigma(\eta)$  of the sample (left axis, colour), again for c) GP and d) GP(R) methods. The rank of the reference FMO structure (right axis) is shown with a thick black line.

Fig. (3c) shows the high ranking of the reference structure amongst our sample of *ersatzs*, which exhibits a sizeable variation of transport efficiencies. A partial explanation for this lies in the tendency for our physically-plausible GPs to generate structures with  $M_i$  larger than that of the FMO, coupled with the negative correlation between  $M_i$  and transport efficiency.<sup>37</sup>

Delving deeper into the structure-dynamics relationship, a closer visual inspection of the top ten performing structures all feature a BChl directly between source and drain, while the bottom ten did not have this feature. This caused us to investigate the contribution of the chromophore closest to the transport vector. We call this the ‘key’ chromophore, with index  $\ddagger$ . In our sample each distinct chromophore assumed this role with approximately equal frequency. This step allowed us to uncover some stronger correlations with  $M_i^{(\ddagger)} \equiv (r_i^{(\ddagger)})^2$  of rel-

ative importance up to  $\sim 3.5\times$  but generally decreasing over time, as shown in Fig. (2e).

But does the combination of a) the strength of correlation between  $M_i$  and  $\eta_i$  and b) the bias in  $M_i$  of our sample of *ersatzs* (with respect to the reference  $M_1$ ) completely explain the high ranking of the reference structure? We address this by studying a sample GP(R) where only rotations are allowed. For these *ersatzs*, the structures are equally compact<sup>38</sup> (Fig. 2a)), but Fig. (3d) shows that the reference still ranks highly. We therefore posit that there is some aspect of the relative orientation of the BChls that is also tuned up for transport.

Investigating this further requires us to probe the structure at a finer level. We adopt an hierarchical approach by fixing variables where we have found a correlation (i.e.  $M_i \rightarrow M_1$ ) before investigating the next variable. This way, we avoid marginalising over the correlations that are known to exist, which would otherwise wash out the evidence of further correlations. Define the total dipole orientation

$$DO_i = \sum_j |\mathbf{d}_j^{(i)} \cdot \mathbf{A}|, \quad (8)$$

as the sum of projections of the  $Q_y$  transition dipole moment  $\mathbf{d}_j$  of each BChl<sup>39</sup> onto the transport vector  $\mathbf{A}$ .  $DO_i$  is zero(one) when the dipoles are perpendicular (parallel or antiparallel) to the transport vector. Fig. (2f) shows a positive correlation  $\mathcal{S}(DO_i, \eta_i(t))$  which again increases (by up to  $\sim 3.3\times$ ) when we select only the key chromophore in Eq. (8) – i.e.  $DO_i^{(\ddagger)}$ .

Fig. (2b) shows that the reference structure has a slightly larger than average  $DO_i$ , which could partially explain its high rank independently of the considerations of moment of inertia. Another likely reason that the reference may be so highly ranked is our conditioning on natural FMO energies. We made a sample where the couplings  $V_{mn}^{(i)}$  are fixed, but energies  $\epsilon_l$  are chosen randomly, finding  $\mathcal{R}(t) \approx 0.5$ . Given the energy distribution  $\epsilon_l$  of the natural FMO, its structure is highly attuned; but given its structure, the energy distribution is not attuned. This hints at improvements that may be possible through on-site energy changes



alone. The correlations found in this work are statistically reliable and significant: we demonstrate this in the supplementary information using (respectively) convergence diagnostics and a p-value analysis.

## Discussion

We have performed a statistical analysis of a large sample of physically-plausible chromophore structures, and succeeded in extracting significant correlations between their structural properties and the time-resolved efficiency with which they transport excitons. We found that compact structures tend to exhibit higher efficiency, and among those, efficiency tended to be higher in structures whose chromophores have their transition dipole aligned with the vector pointing from source to drain. Furthermore, we provide compelling evidence that one chromophore in particular has a dominating influence on the transport efficiency – namely the chromophore that is closest to this vector. The most influential structural property is actually the orientation of this key chromophore, although it becomes less dominant after around 100 fs. These insights could allow for improvements in the transport properties of genetically engineered excitonic networks.<sup>40</sup> Lastly, since our reference structure – that of the natural FMO – is very compact and has moderately well-aligned chromophores, it has a remarkably high efficiency when compared to the other structures we generated. Although these structural properties go some way to explaining the high performance, they most likely do so in combination with energetic considerations – namely the on-site energies of the network (which we were not able to perturb in the same physically-plausible sense as the couplings).

Our geometric perturbation approach places the natural FMO close to the top of the class, with advantages of the order of 20pp (percentage point) increase in transport efficiency around 4 ps ( $\mathcal{R}_\eta(4\text{ps}) = 0.991$ , or 466th of 50,000). This is perhaps more surprising than the striking ranking of light harvesting complexes in purple bacteria, where the 5.5 s.d. advantage may be attributed to the high symme-

try of the chromophore structure,<sup>18</sup> a property that the FMO does not ostensibly possess. Conclusions such as these (based on changes in physical space) are at odds with those inferred from other methodologies of generating *ersatzs*,<sup>17,20</sup> such as uncorrelated matrix-element-perturbation (UMEP) methods. These work by perturbing the Hamiltonian directly in the Hilbert space (see supplementary information) and rank the natural FMO as generic with  $\mathcal{R} \approx 0.5$  (see supplementary information). Given the lack of assured physical plausibility, the necessity of choosing small deviations, and the difficulty of discovering inherent biases, we view the insights gleaned from these methodologies to be of limited relevance to the question of whether natural structures are attuned.

Follow-up research may proceed along several directions: i) running a more sophisticated optimisation routine (such as those that simulate evolutionary processes<sup>12</sup>) to find high performing structures, rather than the simple random search exhibited above; ii) more powerful, machine-powered pattern-finding could be leveraged<sup>13</sup> to seek structural motifs that correlate more strongly with desired transport properties than the rudimentary measures we chose; iii) applying our methodology to alternative pigment-protein complexes or solid state energy transfer materials might reveal other (distinct) structure-dynamics relationships. Lastly, it may be possible to invert the structure-dynamics link in order to estimate unknown structures from measurements of excited-state dynamics (e.g. those probed with ultrafast spectroscopy<sup>41</sup>), potentially complementing other theoretical techniques that explore a structure-spectrum link.<sup>42</sup>

**Acknowledgement** G.C.K. was supported by the Royal Commission for the Exhibition of 1851, P.R. by UK EPSRC, A.T. by ERC (Grant No. 615834), and AD by UK EPSRC (EP/K04057X/2) This work benefited from the Monash Warwick Alliance. The authors thank Martin Plenio, Felix Pollock and Kavan Modi for interesting discussions.

# References

- (1) Blankenship, R. *Molecular Mechanisms of Photosynthesis*; Wiley, 2014.
- (2) Panitchayangkoon, G.; Hayes, D.; Fransted, K. A.; Caram, J. R.; Harel, E.; Wen, J.; Blankenship, R. E.; Engel, G. S. Long-lived quantum coherence in photosynthetic complexes at physiological temperature. *Proceedings of the National Academy of Sciences* **2010**, *107*, 12766–12770.
- (3) Scholes, G. D. Quantum-Coherent Electronic Energy Transfer: Did Nature Think of It First? *The Journal of Physical Chemistry Letters* **2010**, *1*, 2–8.
- (4) Engel, G. S.; Calhoun, T. R.; Read, E. L.; Ahn, T.-K.; Mancal, T.; Cheng, Y.-C.; Blankenship, R. E.; Fleming, G. R. Evidence for wavelike energy transfer through quantum coherence in photosynthetic systems. *Nature* **2007**, *446*, 782–786.
- (5) Collini, E.; Wong, C. Y.; Wilk, K. E.; Curmi, P. M. G.; Brumer, P.; Scholes, G. D. Coherently wired light-harvesting in photosynthetic marine algae at ambient temperature. *Nature* **2010**, *463*, 644–647.
- (6) Huelga, S.; Plenio, M. Vibrations, quanta and biology. *Contemporary Physics* **2013**, *54*, 181–207.
- (7) Ishizaki, A.; Fleming, G. R. Quantum Coherence in Photosynthetic Light Harvesting. *Annual Review of Condensed Matter Physics* **2012**, *3*, 333–361.
- (8) Wilkins, D. M.; Dattani, N. S. Why Quantum Coherence Is Not Important in the Fenna–Matthews–Olsen Complex. *Journal of Chemical Theory and Computation* **2015**, *11*, 3411–3419.
- (9) Duan, H.-G.; Prokhorenko, V. I.; Cogdell, R.; Ashraf, K.; Stevens, A. L.; Thorwart, M.; Miller, R. J. D. Nature does not rely on long-lived electronic quantum coherence for photosynthetic energy transfer. <http://arxiv.org/abs/1610.08425v1> **2016**,
- (10) Baghbanzadeh, S.; Kassal, I. Distinguishing the roles of energy funnelling and delocalization in photosynthetic light harvesting. *Phys. Chem. Chem. Phys.* **2016**, *18*, 7459–7467.
- (11) Schlau-Cohen, G. S. Principles of light harvesting from single photosynthetic complexes. *Interface Focus* **2015**, *5*.
- (12) Scholak, T.; Wellens, T.; Buchleitner, A. Optimal networks for excitonic energy transport. *Journal of Physics B: Atomic, Molecular and Optical Physics* **2011**, *44*, 184012.
- (13) Mostarda, S.; Levi, F.; Prada-Gracia, D.; Mintert, F.; Rao, F. Structure–dynamics relationship in coherent transport through disordered systems. *Nat Commun* **2013**, *4*.
- (14) Zech, T.; Mulet, R.; Wellens, T.; Buchleitner, A. Centrosymmetry enhances quantum transport in disordered molecular networks. *New Journal of Physics* **2014**, *16*, 055002.
- (15) Jesenko, S.; Žnidarič, M. Optimal number of pigments in photosynthetic complexes. *New Journal of Physics* **2012**, *14*, 093017.
- (16) Mohseni, M.; Shabani, A.; Lloyd, S.; Omar, Y.; Rabitz, H. Geometrical effects on energy transfer in disordered open quantum systems. *The Journal of Chemical Physics* **2013**, *138*, 204309.
- (17) Baker, L. A.; Habershon, S. Robustness, efficiency, and optimality in the Fenna–Matthews–Olsen photosynthetic pigment-protein complex. *The Journal of Chemical Physics* **2015**, *143*.
- (18) Baghbanzadeh, S.; Kassal, I. Geometry, Supertransfer, and Optimality in the Light Harvesting of Purple Bacteria. *The Journal of Physical Chemistry Letters* **2016**, *7*, 3804–3811.



- (19) Mohseni, M.; Rebentrost, P.; Lloyd, S.; Aspuru-Guzik, A. Environment-assisted quantum walks in photosynthetic energy transfer. *The Journal of Chemical Physics* **2008**, *129*.
- (20) Caruso, F.; Chin, A. W.; Datta, A.; Huelga, S. F.; Plenio, M. B. Highly efficient energy excitation transfer in light-harvesting complexes: The fundamental role of noise-assisted transport. *The Journal of Chemical Physics* **2009**, *131*.
- (21) Schijven, P.; Kohlberger, J.; Blumen, A.; Mülken, O. Modeling the quantum to classical crossover in topologically disordered networks. *Journal of Physics A: Mathematical and Theoretical* **2012**, *45*, 215003.
- (22) Caruso, F. Universally optimal noisy quantum walks on complex networks. *New Journal of Physics* **2014**, *16*, 055015.
- (23) Li, Y.; Caruso, F.; Gauger, E.; Benjamin, S. C. ‘Momentum rejuvenation’ underlies the phenomenon of noise-assisted quantum energy flow. *New Journal of Physics* **2015**, *17*, 013057.
- (24) Fenna, R. E.; Matthews, B. W. Chlorophyll arrangement in a bacteriochlorophyll protein from *Chlorobium limicola*. *Nature* **1975**, *258*, 573–577.
- (25) Löhner, A.; Ashraf, K.; Cogdell, R. J.; Köhler, J. Fluorescence-excitation and Emission Spectroscopy on Single FMO Complexes. *Scientific Reports* **2016**, *6*, 31875.
- (26) Moix, J.; Wu, J.; Huo, P.; Coker, D.; Cao, J. Efficient Energy Transfer in Light-Harvesting Systems, III: The Influence of the Eighth Bacteriochlorophyll on the Dynamics and Efficiency in FMO. *The Journal of Physical Chemistry Letters* **2011**, *2*, 3045–3052.
- (27) Tronrud, D. E.; Wen, J.; Gay, L.; Blankenship, R. E. The structural basis for the difference in absorbance spectra for the FMO antenna protein from various green sulfur bacteria. *Photosynthesis Research* **2009**, *100*, 79–87.
- (28) The Protein Data Bank (entry 3EOJ). <http://www.rcsb.org/pdb/explore/explore.do?structureId=3EOJ>.
- (29) Berman, H. M.; Westbrook, J.; Feng, Z.; Gilliland, G.; Bhat, T. N.; Weissig, H.; Shindyalov, I. N.; Bourne, P. E. The Protein Data Bank. *Nucleic Acids Research* **2000**, *28*, 235–242.
- (30) Curutchet, C.; Mennucci, B. Quantum Chemical Studies of Light Harvesting. *Chemical Reviews* **2017**, *117*, 294–343.
- (31) Madjet, M. E.; Abdurahman, A.; Renger, T. Intermolecular Coulomb Couplings from Ab Initio Electrostatic Potentials: Application to Optical Transitions of Strongly Coupled Pigments in Photosynthetic Antennae and Reaction Centers. *The Journal of Physical Chemistry B* **2006**, *110*, 17268–17281.
- (32) Chenu, A.; Scholes, G. D. Coherence in energy transfer and photosynthesis. *Annual review of physical chemistry* **2015**, *66*, 69–96.
- (33) Breuer, H.; Petruccione, F. *The Theory of Open Quantum Systems*; OUP Oxford, 2007.
- (34) Misra, B.; Sudarshan, E. C. G. The Zeno’s paradox in quantum theory. *Journal of Mathematical Physics* **1977**, *18*, 756–763.
- (35) Rebentrost, P.; Mohseni, M.; Aspuru-Guzik, A. Role of Quantum Coherence and Environmental Fluctuations in Chromophoric Energy Transport. *The Journal of Physical Chemistry B* **2009**, *113*, 9942–9947.
- (36) Kassal, I.; Yuen-Zhou, J.; Rahimi-Keshari, S. Does Coherence Enhance Transport in Photosynthesis? *The Journal of Physical Chemistry Letters* **2013**, *4*, 362–367.

- (37) We made a new sample with much stricter constraints on the moment of inertia (removing the bias), and the reference FMO continued to perform well there (see supplementary materials).
- (38) The moment of inertia is only approximately constant when we perform only rotations of the chromophores. This is because we rotate chromophores around their geometric centroids, but calculate moment of inertia with the central Magnesium atom. These two points are slightly displaced with respect to each other ( $\sim 0.312\text{\AA}$ ).
- (39) Milder, M. T. W.; Brüggemann, B.; van Grondelle, R.; Herek, J. L. Revisiting the optical properties of the FMO protein. *Photosynthesis Research* **2010**, *104*, 257–274.
- (40) Park, H.; Heldman, N.; Rebentrost, P.; Abbondanza, L.; Iagatti, A.; Alessi, A.; Patrizi, B.; Salvalaggio, M.; Bussotti, L.; Mohseni, M. et al. Enhanced energy transport in genetically engineered excitonic networks. *Nat Mater* **2016**, *15*, 211–216.
- (41) Yuen-Zhou, J.; Krich, J.; Kassal, I.; Aspuru-Guzik, A.; Johnson, A. *Ultrafast Spectroscopy: Quantum Information and Wavepackets*; IOP expanding physics; Institute of Physics Publishing, 2014.
- (42) Chenu, A.; Cao, J. Construction of Multichromophoric Spectra from Monomer Data: Applications to Resonant Energy Transfer. *Phys. Rev. Lett.* **2017**, *118*, 013001.